HHS Public Access

Author manuscript

Biomaterials. Author manuscript; available in PMC 2021 August 01.

Published in final edited form as:

Biomaterials. 2020 August ; 249: 120011. doi:10.1016/j.biomaterials.2020.120011.

Fucoidan functionalization on poly(vinyl alcohol) hydrogels for improved endothelialization and hemocompatibility

Yuan Yao[1], **Aung Moe Zaw**[1], **Deirdre E. J. Anderson**[2], **Monica T. Hinds**[2], **Evelyn K. F. Yim**[1,3,4,*]

[1]Department of Chemical Engineering, University of Waterloo, 200 University Avenue West, Waterloo, ON, Canada N2L 3G1

[2]Department of Biomedical Engineering, Oregon Health & Science University, Portland, OR, USA 97239

[3]Waterloo Institute for Nanotechnology, University of Waterloo, 200 University Avenue West, Waterloo, ON, Canada N2L 3G1

[4]Center for Biotechnology and Bioengineering, University of Waterloo, 200 University Avenue West, Waterloo, ON, Canada N2L 3G1

Abstract

The performance of clinical synthetic small diameter vascular grafts remains disappointing due to the fast occlusion caused by thrombosis and intimal hyperplasia formation. Poly(vinyl alcohol) (PVA) hydrogels have tunable mechanical properties and a low thrombogenic surface, which suggests its potential value as a small diameter vascular graft material. However, PVA does not support cell adhesion and thus requires surface modification to encourage endothelialization. This study presents a modification of PVA with fucoidan. Fucoidan is a sulfated polysaccharide with anticoagulant and antithrombotic properties, which was shown to potentially increase endothelial cell adhesion and proliferation. By mixing fucoidan with PVA and co-crosslinked by sodium trimetaphosphate (STMP), the modification was achieved without sacrificing mechanical properties. Endothelial cell adhesion and monolayer function were significantly enhanced by the fucoidan modification. *In vitro* and *ex-vivo* studies showed low platelet adhesion and activation and decreased thrombin generation with fucoidan modified PVA. The modification proved to be compatible with gamma sterilization. *In vivo* evaluation of fucoidan modified PVA grafts in rabbits exhibited increased patency rate, endothelialization, and reduced intimal hyperplasia formation. The fucoidan modification presented here benefited the development of PVA vascular grafts and can be adapted to other blood contacting surfaces.

[*]**Corresponding author**: Evelyn K.F. Yim, Department of Chemical Engineering, University of Waterloo, 200 University Avenue West, Waterloo, ON, Canada N2L 3G1 eyim@uwaterloo.ca.

Data Availability

The experimental data required to reproduce the findings from this study will be made available to interested investigators upon request.

Keywords

small diameter vascular graft; fucoidan; endothelialization; hemocompatibility; rabbit carotid artery; end-to-side anastomosis

1. Introduction

Vascular diseases remain the leading cause of death globally. Autologous artery or vein grafts are used to bypass or replace occluded blood vessels to restore blood flow, but their availability is limited. Synthetic vascular grafts have been an alternative to autologous grafts for a long time and benefited millions of patients. Commercially available synthetic vascular grafts, such as ePTFE and Dacron®, showed satisfactory long-term performance for larger diameter vessels (>6 mm), but displayed inferior performance in small-diameter applications (<6mm).[1–3] Yet at small diameter, these synthetic grafts occlude either rapidly subsequent to surgery due to acute thrombosis formation or subsequently due to substantial intimal hyperplasia development in the lumen of vascular grafts and at the anastomoses sites, both of which were speculated to be caused by the lack of functional endothelial coverage.[4, 5] To improve endothelialization, surface modification of synthetic materials is frequently carried out with different strategies. Anticoagulant and antiplatelet coating and conjugations are the most common approaches. Trials using heparin on artificial graft materials have shown suppressed thrombin generation and improved patency rates in animal studies.[6–8] However, the hemorrhagic effect of heparin raises additional concerns.

Fucoidan is a sulfated polysaccharide isolated from brown algae and has been extensively studied in the past decades for its various biological activities, including anticoagulant, anti-inflammatory, antioxidant, and anticancer properties.[9–11] Despite anticoagulant and antithrombotic activities similar to heparin, fucoidan does not cause hemorrhagic effects, [12] making it a promising alternative to heparin. Furthermore, the potentials in promoting endothelial cell growth [13] and suppressing smooth muscle cell proliferation [14] combine to make fucoidan a promising surface modification molecule for synthetic vascular grafts.

Poly (vinyl alcohol) is a synthetic biocompatible polymer and has been studied for various biomedical applications. PVA crosslinked by sodium trimetaphosphate (STMP), a food grade crosslinker, was shown to be potentially appropriate for small diameter vascular graft application. Our previous studies found STMP-crosslinked PVA has tunable mechanical properties that can match native blood vessels.[15, 16] However, the main barrier for developing PVA small diameter vascular grafts is the absence of endothelialization on PVA due to the hydrophilicity and lack of cell binding sites. Our group and other groups have been investigating surface modification strategies to improve the endothelialization of PVA, including plasma treatment,[17, 18] surface topographical patterning,[19] and peptide and protein coating.[20–22] However, developing a modification method that both improves endothelialization and maintains a non-thrombogenic surface is still challenging.

In the present study, we hypothesized that modification of PVA with fucoidan could improve endothelialization without compromising the desirable blood compatibility of PVA. Previous studies using fucoidan to promote endothelialization required the presence of supplementary

molecules, such as growth factors and extracellular proteins, or some required multi-layer coating to achieve best performance. [23–25] Our current study employed fucoidan alone without any supplementary molecules, and the modification was carried out with a mild and simple procedure by mixing fucoidan in aqueous PVA solution followed by STMP crosslinking in ambient conditions. Human vascular endothelial cell adhesion and function on fucoidan modified PVA were studied by characterizing cell density, cell monolayer formation, and cell marker expression. Platelet adhesion, activation, and thrombosis were assessed *in vitro* using rabbit blood and *ex-vivo* in a non-human primate shunt model. Furthermore, we tested the *in vivo* performance of fucoidan modified small diameter PVA grafts in a rabbit carotid artery model. *In situ* endothelialization, patency rate, and restenosis of the grafts were analyzed. Overall, the study highlights the potential of the fucoidan modification to improve endothelialization without compromising the hemocompatibility and will aid in the development of durable PVA small diameter vascular grafts and other vascular prostheses.

2. Materials and methods

2.1 Preparation of PVA hydrogels

PVA hydrogels were prepared as previously published.[19] In brief, an aqueous solution of 10% PVA solution was prepared by dissolving PVA powder (average Mw 85,000–124,000, 87%−89% hydrolyzed, Sigma-Aldrich) in deionized (DI) water, followed by autoclaving at 121 °C for 20 min to facilitate dissolving. To crosslink PVA, 15% (w/v) STMP solution was mixed with 10% PVA solution, and 30% (w/v) NaOH was added dropwise to activate the functional groups of PVA and STMP. The obtained solution was either cast on petri dishes to form PVA films or dip-coated on cylinder molds to form tubular grafts. PVA films and tubular grafts were then kept in a cabinet with controlled temperature (20°C) and humidity (60%−70%) until fully crosslinked. Solutions of 10X phosphate buffer solution (PBS), 1X PBS, and DI water were used to rehydrate and de-mold crosslinked PVA hydrogels.

To modify PVA hydrogels, fucoidan (crude, from *Fucus vesiculosus*, Sigma-Aldrich) was mixed with 10% PVA solution (PVA:fucoidan = 30:1 (w/w)) prior to adding STMP and stirred for 24 hours to homogenize. The fucoidan-PVA mixture was then co-crosslinked by STMP as described above (PVA-F).

2.2 Sterilization of PVA hydrogels

PVA and PVA-F tubular grafts were sterilized by gamma irradiation before implantation, as previously reported[26]. The gamma sterilization was done at Southern Ontario Centre for Atmospheric Aerosol Research in University of Toronto. The irradiation was carried out with a Co-60 source (G.C. 220) at a dose of 25 kGy.

2.3 Scanning electron microscope (SEM) measurement

The PVA and PVA-F samples were dried overnight and mounted on aluminum stubs and imaged by a high-resolution field emission scanning electron microscope (Zeiss 1550) with energy dispersive X-ray (EDX) spectroscopy (Oxford Instruments) in high vacuum mode at 10 kV. No coating was applied prior to imaging.

2.4 Static water contact angle (WCA) measurement

Water contact angle of PVA and PVA-F films were measure with a JC2000D3 contact angle meter. A 2 μl water drop was deposited onto the hydrated PVA films, and images were captured after the droplet remained stable on the PVA surfaces. The angle value was calculated using ImageJ.

2.5 Fucoidan concentration determination

The density of fucoidan on PVA-F films were determined by using a metachromatic dye, toluidine blue O (TBO) (Sigma-Aldrich), adopted from a previous published procedure[27]. A 1 cm^2 film of PVA and PVA-F were immersed in 500 μl of TBO solution with a concentration of 50 μg/ml and shaken for 1 hr. The absorbance at 631 nm of the supernatant was then measured using Synergy 4 multi-detection microplate reader (BioTek). To quantify the density of fucoidan on PVA-F samples, a calibration curve (as shown in Fig S1) was generated from free fucoidan solutions with a concentration range from 1.0 μg/ml-1.0 mg/ml. Hexane was added to the free fucoidan solution to remove the fucoidan-toluidine blue complex from the aqueous phase before reading the absorbance. To evaluate stability of the modification, PVA-F samples were stored in PBS at 37 °C for 15 days, 30 days and 60 days, and the density of fucoidan was compared against freshly prepared PVA-F samples.

2.6 Crosslinking density measurement

Crosslinking density of PVA and PVA-F hydrogels was determined by measuring phosphate concentration with a phosphate assay kit (Abcam). Briefly, around 200 mg of the hydrogel was degraded in 10% nitric acid at 105°C for 1 hour. The solution was diluted with double distilled water. An aliquot of 200 μl sample was then mixed with 30 μl phosphate reagent and incubated for 30 min at room temperature protected from light. The phosphate concentration was measured at 650 nm wavelength using different concentrations of phosphoric acid solutions as standards.

2.7 Water content measurement

Hydrated PVA and PVA-F hydrogels were weighed to get initial weight, W_H. The samples were then dehydrated in 60°C oven until reaching stable weight, W_D. The water content was determined by equation: Water content = $(W_H - W_D)/W_H \times 100\%$.

2.8 Mechanical property test

Compliance test of PVA and PVA-F grafts was carried out by measuring outer diameter change of the grafts at 80 mmHg (D_{80}) and 120 mmHg (D_{120}) internal pressure. Grafts were clamped at one end and the other end was connected to a bag of saline solution through a catheter. The inner pressure of 80 mmHg and 120 mmHg were achieved by changing the height of the saline bag. The diameters of the graft with different inner pressures were measured and the compliance was calculated by Compliance (%/40mmHg) = $(D_{120}\text{-}D_{80})/D_{80} \times 100\%$. Burst pressure was measured by exposing the grafts to increasing intramural pressure until failure. A segment of the graft was clamped at one end and the other end was linked to a nitrogen gas cylinder through a catheter. A pressure regulator was used to control the pressure supply. Uniaxial tensile tests were measured using a Universal Mechanical

Tester (UNMT-2MT, T1377, Center for Tribology, Inc.) at an extension rate of 10 mm/min with a load cell of 10 kg for circumferential test and 100 kg for longitudinal test. The cross-sectional area of the sample was measured by ImageJ.

2.9 Endothelial cell adhesion and function assay

Human umbilical vein endothelial cells (HUVECs, passage 3–5, Lonza) were maintained in EGM-2MV medium (Lonza) and seeded on PVA, PVA-F, and glass coverslips with a seeding density of 50,000 cells/cm^2. Cells were cultured for either 2 days until confluent for cell functional marker staining or 24 hours until sub-confluent for extracellular matrix (ECM) protein staining. Cells were fixed with 4% paraformaldehyde (PFA), permeabilized with 0.1% Triton X-100, and blocked with 5% goat serum and 0.3% Triton X-100. Following blocking, the cells were immune-stained with platelet endothelial cell adhesion molecule (PECAM-1, mouse-anti-PECAM-1 at 1:100, monoclonal, Abcam, ab9498), vascular endothelial cadherin (VE-Cad, rabbit anti-VE-Cad at 1:100, polyclonal, Cell Signaling Technology, 2158S), endothelial NOS (eNOS, mouse anti-eNOS at 1:100, monoclonal, Abcam, ab76198), collagen IV antibody (rabbit anti-collagen IV at 1:100, polyclonal, Abcam, ab6586), or laminin antibody (rabbit anti-laminin at 1:100, polyclonal, Alfa Aesar, J65295) with the corresponding AlexaFluor labeled secondary goat antibodies, and counterstained with DAPI to label nuclei. Images were taken using Zeiss fluorescence microscope (Axio Observer Z1) and analyzed using ImageJ software.

2.10 *In vitro* hemocompatibility test

In vitro hemocompatibility was performed on flat samples by incubating samples with rabbit platelet rich plasma (PRP) under orbital shaking condition. Briefly, blood samples were collected from healthy male New Zealand rabbits in polypropylene tubes and primed with 3.8% sodium citrate (1ml per 9 ml blood). Whole blood was centrifuged at 200 g for 10 min to collect PRP. 200 μl of PRP was then incubated on PVA and PVA-F samples for 1 h on an orbital shaker at 200 rpm. Glass coverslips, coated with 500 μl of 0.1 mg/ml bovine collagen type I, were included as positive control, while ePTFE grafts with carbon lining (CARBOFLO®, Bard) were cut open to expose the lumen and used as a negative control. Non-adherent PRP solution was subsequently collected for a real-time thrombin generation assay, while the adhered platelets on PVA samples were washed with ice-cold PBS to remove unattached red blood cells and platelets, and then kept for either SEM or a lactate dehydrogenase (LDH) assay.

Adhered platelets on PVA were fixed with 2.5% glutaraldehyde in PBS for 20 min, and then gradually dehydrated using increasing ethanol concentration. Dehydrated samples were left to dry at room temperature before SEM imaging. To quantify platelets adhered on PVA samples, adherent platelets were lysed with 1% Triton X-100 by incubating at 37°C for 1 hour. The lysate was analyzed with LDH kit (Roche) and the absorbance was measured with a microplate reader at 490 nm.

Realtime thrombin generation assay was done with Technothrombin® Thrombin Generation Assay (TGA) kit (Diapharma) according to the manufacturer's protocol. In brief, after a 1-hour incubation, PRP was collected and diluted with supplied buffer. 40 μl of PRP dilution

was added into a 96 well plate, and 50 μl of supplied substrate was added to each sample to initiate the thrombin reaction. The supernatant fluorescence (390 nm/460 nm) was measured by the plate reader for 2 hours at 37°C. According to the thrombin generation curve, the starting time of the thrombin generation (Lagtime), maximum thrombin generation rate (Peak), and total amount of generated thrombin (ETP) were analyzed by the manufacturer provided software.

2.11 *Ex vivo* shunt assay

Ex-vivo hemocompatibility test was done on tubular samples with whole blood under flow condition in a non-human primate *ex-vivo* shunt model. PVA tubular grafts, 4 mm diameter and 5 cm in length, were tested in a flowing, whole blood model of thrombosis as described previously.[22] Four juvenile, baboons (Papio Anubis) had a chronic, arteriovenous shunt with radiolabeled platelets and fibrin. The graft was placed between silicone tubing extensions to test over a Brivo NM615 nuclear imaging camera (GE) with 1 hour of blood flow, controlled at 100 mL/min without any antiplatelet therapies. Platelet accumulation was tested dynamically during this time while fibrin accumulation was quantified at the end of the study. PVA samples (n=4–8 per group) were tested along with a collagen-coated expanded polytetrafluoroethylene (ePTFE, n=2) positive control and a clinical ePTFE control (W.L. Gore, n=2). Platelet data were analyzed using a multi-way repeated measures linear mixed effects model against PVA type and time. In order to increase model precision a fractional polynomial term (time × ln(time)) and all relevant interactions were added as model fixed effects. Fibrin data were tested for normality using a q-q plot and homogeneity of variance with a Levene's test. After determining that these data failed these ANOVA assumptions, fibrin and platelet data were natural log transformed, with 0.01 added to each value to avoid exclusion of any zero values.

Patency in the *ex vivo* shunt model was measured as described previously.[28] In brief, samples were fixed with 3.7% paraformaldehyde, rinsed, and rendered radiopaque. Samples were imaged using X-ray microcomputed tomography (microCT). Data was imported into Amira® and the luminal volume was quantified. This volume was divided by the sample length to give the average luminal area. These data were analyzed with a one-way ANOVA to compare only the three PVA test samples. Luminal area data were also tested for normality and homogeneity but did not fail the ANOVA assumptions and therefore were not transformed.

These studies were approved by the Oregon National Primate Research Center (ONPRC) Institutional Animal Care and Use Committee. Baboons were cared for at ONPRC according to the "Guide to the Care and Use of Laboratory Animals" prepared by the Committee on Care & Use of Laboratory Animals of the Institute of Laboratory Animal Resources, National Research Council (International Standard Book, Number 0-309-05377-3, 1996).

2.12 Implantation of fucoidan modified small diameter vascular grafts

Implantation of the small diameter vascular grafts was done as previously published.[29] Briefly, New Zealand White rabbits (male, weight 3.5–4.0 kg, Charles River laboratories) were anaesthetized by giving 400–800 ml/min oxygen and gas isoflurane (1–3%) through

endotracheal intubation. Heparin (200 IU/kg) was given intravenously prior to arterial clamping. Segments (2 cm) of unmodified PVA grafts (n=5) and PVA-F grafts (n=6) with inner diameter of 1.7 mm (parameters are as shown in Table S1) were anastomosed onto the right carotid artery, with end-to-side anastomosis, using 8–0 Nylon suture (AD Surgical). Aspirin (15 mg/kg) was administered post-surgery until endpoint. ePTFE grafts (2 cm, n=4, Zeus) with 2 mm inner diameter were included as positive controls. Ultrasound doppler imaging and measurements were done using SonixTouch (Analogic Ultrasound, Peabody) and 10.0 MHz probe at midpoints (14 days) and endpoints (28–31 days) to detect blood flow and check graft patency. At endpoint, rabbits were euthanized with sodium pentobarbital (100 mg/kg). The grafts altogether with native arteries and corresponding left carotid arteries were explanted and fixed in 4% PFA for 72 hours. The fixed grafts were serially dehydrated, parafilm embedded, and sectioned in the middle of the grafts and at the proximal and distal anastomoses. H&E, immunohistochemistry and immunofluorescence staining were carried out to measure luminal patent area, analyze intimal hyperplasia and detect endothelial cells, respectively.

All rabbit studies were approved (#AUPP 16–09) by the Animal Care Committee according to the Canadian Council on Animal Care's Guidelines, the requirements of Province of Ontario's Animals for Research Act, and the University of Waterloo's Guidelines for the Use of Animals in Research and Teaching.

2.14 Statistics

Statistical analysis of *ex-vivo* shunt study was stated as above. Other statistical analysis was performed using GraphPad Prism 7. The values of all data were presented as mean ± Standard Deviation (SD). To determine statistical significance, t-test, one-way ANOVA test with Tukey's *post hoc* test and two-way ANOVA with Sidak's *post hoc* test were used. Statistical significance criterion was set at p value of <0.05.

3 Results

3.1 Characterization of fucoidan modified PVA hydrogels

The fucoidan modification of PVA was achieved by mixing fucoidan into PVA solution and co-crosslinked by STMP, as shown in Fig 1A. SEM images showed the structures on the surface of PVA and PVA-F hydrogels (Fig 1B). The unmodified PVA hydrogels had a smooth surface, while PVA-F hydrogels exhibited irregular structures on the surfaces. Surface energy of PVA and PVA-F was determined by measuring static water contact angle. PVA-F surface showed a slightly lower water contact angle possibly due to the hydrophilicity of fucoidan (Fig 1C). The presence of fucoidan on PVA-F was visually verified from the purple color change of toluidine blue staining, as shown in Fig 1D. Fucoidan density on PVA-F samples was quantified to be an average of 53.4±2.0 μg/cm^2. PVA-F films were stored in PBS at 37°C for up to 60 days to determine to stability of fucoidan modification. Fucoidan density after incubation for 15 days, 30 days and 60 days was 43.5±15.4 μg/cm^2, 42.2±12.4 μg/cm^2 and 36.8±5.5 μg/cm^2, respectively. No significant differences of fucoidan density were observed over time (p=0.3025) (Fig 1E). EDX was also

carried out to analyze the element composition on PVA-F samples. The atomic percentage of sulfur is 0.12±0.03%, confirming the presence of fucoidan (Fig S2).

3.2 Biomechanical properties of fucoidan modified PVA hydrogels

PVA-F showed significantly higher phosphate content (Fig 2A), indicating a significantly higher crosslinking density. Water content of PVA-F hydrogels (66.07±1.69%) was not significantly different from unmodified PVA hydrogels (64.27±2.22%) (Fig 2B).

Mechanical properties of PVA and PVA-F hydrogels were characterized. Compliance was determined *in vitro* by measuring the diameter increase of PVA and PVA-F tubular grafts from 80 mmHg to 120 mmHg internal pressure. PVA and PVA-F grafts had a compliance of 1.63±0.15 (%/40 mmHg) and 1.73±0.10 (%/40 mmHg), respectively (Fig 2C). With higher crosslinking density, PVA-F hydrogels were significantly stronger with a burst pressure of 831.50±75.43 mmHg, while unmodified PVA hydrogels had a burst pressure of 752.55±56.16 mmHg (Fig 2D, $p<0.05$, n=3). The tensile Young's modulus of PVA and PVA-F hydrogels were measured in both longitudinal and circumferential directions. Longitudinal Young's modulus for PVA hydrogels was 1.28±0.25 MPa and was increased to 1.57±0.29 MPa for PVA-F hydrogels (Fig 2E). Similarly, the circumferential Young's modulus was higher for PVA-F hydrogels (1.22±0.09 MPa) compared to PVA hydrogels (1.08±0.03 MPa) (Fig 2F), and a significant increase was observed ($p<0.05$, n=3).

3.3 Endothelial cell adhesion on fucoidan modified PVA hydrogels

To evaluate the potential of PVA-F hydrogels for endothelialization, HUVECs adhesion on PVA, PVA-F, and glass coverslips was analyzed. HUVECs exhibited good attachment and spreading and formed confluent monolayers on PVA-F hydrogels and glass coverslips, while only few cells were attached on unmodified PVA hydrogels and failed to form monolayers (Fig 3A and Fig S3). The cell density on PVA-F hydrogels (816 ± 217 cells/mm^2) was significantly higher than that on unmodified PVA (48 ± 16 cells/mm^2, $p<0.0001$), and was comparable to that on glass (965 ± 80 cells/mm^2, $p=0.3076$) (Fig 3B).

HUVECs on all substrates were immuno-stained with CD31 (platelet endothelial cell adhesion molecule, PECAM), VE-Cadherin, and eNOS to examine the cell monolayer function. As shown in Fig 3A and Fig S3, strong eNOS expression was presented from cells on PVA-F and glass coverslips. The CD31 and VE-Cadherin were expressed strongly at the cell boundaries of the HUVECs on PVA-F and glass coverslips, while only in the cell cytoplasm on unmodified PVA. The quantification of protein expression of HUVECs on PVA-F and glass coverslips was as shown in Fig 3C, cells on unmodified PVA were not taken into calculation due to low cell numbers. Cells on PVA-F showed similar CD31 and VE-Cadherin expression levels as those on glass, the eNOS expression on PVA-F was significantly higher than on glass ($p<0.05$). Extracellular matrix protein, collagen IV and laminin, produced by HUVECs were also stained and as shown in Fig 3D. Both collagen IV and laminin were deposited by HUVECs on PVA-F, and the expression levels of both proteins was similar to those on glass coverslips (Fig 3E).

3.4 *In vitro* hemocompatibility of fucoidan modified PVA hydrogels

To examine the platelet behaviors on PVA and PVA-F hydrogels, we performed an LDH assay to measure the platelet adhesion and SEM to examine the morphology of attached platelets. The platelets on collagen coated glass were well spread, while the platelets on PVA and ePTFE were rounded (Fig 4A). More platelets were attached on PVA-F, and the platelets appeared to form more pseudopods compared with those on ePTFE and PVA. The LDH absorbance of collagen coated glass samples was significantly higher than ePTFE, PVA, and PVA-F, but no significant difference was observed among ePTFE, PVA, and PVA-F groups (Fig 4B). The results indicated that fucoidan modification did not increase platelet adhesion or activation.

Thrombogenicity of the PVA-F hydrogels was examined by a real-time thrombin generation assay. As the kinetic thrombin generation curved shows in Fig 4C, thrombin was generated at much faster rate and a larger amount on collagen coated glass compared to ePTFE, PVA, and PVA-F. The quantitative parameters, lagtime, peak, and ETP (Fig 4D–F) confirmed the observation in the kinetic curves. Collagen coated glass had a significantly shorter lagtime, higher peak thrombin generation, and more thrombin generation in total. Also, PVA-F had lower thrombin generation compared to PVA and ePTFE, though no statistical significance was observed.

3.5 Gamma sterilization of fucoidan modified PVA hydrogels

Sterilization is required for implantation. To examine if gamma irradiation would affect the fucoidan modified PVA hydrogels, we compared the compliance, water contact angle, cell adhesion, and thrombin generation of fucoidan modified PVA hydrogels before and after gamma irradiation. Compliance and burst pressure of both PVA and PVA-F grafts were not significantly changed after gamma irradiation (Fig S4). HUVECs attached well on both non-gamma treated (PVA-F) and gamma treated samples (PVA-Fg) (Fig S5), and the cell density was significantly higher on PVA-Fg samples (Fig 5A). Contact angle on both PVA and PVA-F were not significantly changed after gamma irradiation (Fig S6). Moreover, the expression levels of CD31 and eNOS from ECs on PVA-F and PVA-Fg showed no significant difference (Fig 5B and C). The gamma irradiation also did not significantly change the thrombin formation on both unmodified PVA and PVA-F samples (Fig 5D–F). But overall, the properties of PVA-F hydrogels were not significantly altered by the gamma irradiation.

3.6 *Ex-vivo* shunt study of fucoidan-modified PVA grafts

PVA, PVA-F, and PVA-Fg tubular grafts were tested in an *ex-vivo* baboon shunt model, with collagen coated ePTFE grafts and normal ePTFE grafts as controls. The platelets (Fig 6A) fibrin accumulation (Fig 6B), and average luminal patent area (Fig 6C) during the 1-hour testing period did not exhibit any significant differences, though there was a borderline insignificance in platelet accumulation among PVA, PVA-F and PVA-Fg groups ($p=0.0523$). PVA-F and PVA-Fg grafts had the lowest amount of platelet and fibrin accumulation, although after gamma sterilization, PVA-Fg had slightly increased fibrin accumulation, but still lower than PVA and the ePTFE control groups. PVA-Fg had the highest average luminal area.

3.7 *In-vivo* study of fucoidan modified PVA small diameter vascular graft

Sterilized PVAg, PVA-Fg, and ePTFE grafts were implanted in rabbit right carotid arteries. The dimensions of the implanted grafts were shown in Fig 7A. The PVA and PVA-F grafts were 1.7 mm in diameter and 2 cm in length with curvature of 1.4 cm radius in the middle. The ePTFE grafts were straight with 2.0 mm in diameter and 2 cm in length. Parameters of the implanted grafts with comparisons to native arteries were shown in Table S1. The grafts were implanted in an end-to-side anastomotic technique, as shown in Fig 7C. After 1-month implantation, ePTFE (n=4), PVAg (n=5), and PVA-Fg (n=5) grafts had a patency rate of 75%, 40%, and 80%, respectively (Fig 7B). The ultrasound detection showed that PVA-Fg grafts still maintained strong flow after 1 month while PVAg grafts were either occluded or had minimal flow (Fig 7D and Fig S7). It was also observed that the blood flow inside ePTFE grafts had big animal variations (Fig S7).

After 1 month of implantation, the grafts and contralateral native artery were harvested. The grafts were sectioned at the anastomotic sites (P and D) and the middle (M) as shown in Fig S8A, for H&E and immunofluorescent staining. As shown in Fig 8A, the PVA-Fg grafts had a layer of cells on the luminal surfaces, while no cells were presented on plain PVAg surfaces. Immunofluorescent staining showed that the cells on PVA-Fg lumen expressed endothelial cell marker (CD31 and eNOS), indicating endothelial cell coverage on PVA-Fg lumens at both anastomotic sites and middle of the graft (Fig 8B and Fig S8B and C). The ePTFE grafts used in this study had a porous structure, the CD31 and eNOS positive staining in ePTFE graft may likely have come from the endothelial cells trapped inside the porous structures.

The H&E stained cross-sections of the grafts were pictured and the stenosis percentage at the anastomotic junctions was quantified by dividing the area of stenosis to the luminal area of the grafts (Fig 9). PVA-Fg grafts showed a lower percentage of stenosis than PVAg grafts at both proximal and distal anastomotic sites, while the stenosis percentage for ePTFE grafts varied from 10% to 90%. The intimal hyperplasia inside the lumens of ePTFE, PVA and PVA-F grafts all showed α-SMA positive staining (Fig 9D), which indicates the presence of smooth muscle cells in the intimal hyperplasia. Ki67 staining showed the presence of proliferating cells presented in the intimal hyperplasia, but the density of proliferating cells was low (Fig 9E and Fig S9). In general, the PVA-Fg grafts showed a better *in-vivo* performance than plain PVAg grafts and exhibited *in situ* endothelialization.

4. Discussion

Despite decades of development for synthetic vascular grafts, the performance of synthetic vascular grafts with diameters smaller than 6 mm is still disappointing due to the poor patency rate. One of the main reasons for failure is the lack of endothelialization of the synthetic materials, which leads to severe thrombosis formation and intimal hyperplasia formation. Surface modification of synthetic vascular grafts is required to reduce early-stage blood clotting formation and to enhance *in situ* endothelialization for long term patency. Proteins, such as ECM components, and anticoagulants, such as heparin, are frequently used molecules to encourage better vascular graft performance, however, these modifications both cause other complications.[30, 31] Many protein modifications improve the endothelial cell

attachment but at the same time promote platelet attachment and activation,[32–34] which further increases the chance of thrombus formation and graft occlusion. Coating and immobilizing heparin on synthetic vascular grafts has been shown to reduce platelet adhesion and thrombin generation [6, 35–37], but with the risk of hemorrhagic effect and heparin-induced thrombocytopenia.[38, 39] To develop a reliable modification, our work studied the ability of a fucoidan modification to promote endothelial cell adhesion and blood compatibility of PVA hydrogels. Fucoidan was chosen due to its ability to de-activate thrombin and inhibit thrombin generation without causing hemorrhagic effect [12, 40, 41]. Other studies also showed that hydrogels functionalized with fucoidan could dictate the release of vascular endothelial growth factors from the hydrogel and promote re-endothelialization.[23, 24] In our study, fucoidan was used to modify STMP-crosslinked PVA hydrogels. The fucoidan modification of PVA was achieved by simply mixing fucoidan with the PVA solution, and then crosslinked by STMP in the presence of NaOH. Due the viscosity of PVA solution and decreased solubility of fucoidan in a basic solution, the dispersion of fucoidan in PVA solution may not be even, and thus the generated PVA-F hydrogels had rougher surfaces compared to plain PVA. We also observed an uneven distribution of toluidine blue on PVA-F samples under microscope showing accumulation of fucoidan around the circular area (as shown in Fig S10), which further supported our speculation of non-uniform distribution. In addition, the difference of viscosity and solubility may have caused a change in the evaporation rate of water during PVA-F hydrogel fabrication, which would also lead to a rougher surface.[22] Our previous study showed that micro-sized circular structures themselves did not significantly affect HUVECs behaviors. [42] Also, we found that topographies without other biochemical modifications do not support endothelial cells to form monolayers on PVA.[19] Thus, we speculate that the surface roughness of PVA-F was not a significant contributor to the improved endothelialization. Studies have shown that platelets and thrombogenicity can be manipulated by topographies with the same size range as platelets or below.[43] Our previous studies using PVA/gelatin also observed uneven surfaces, but no significant difference of platelets adherent was observed.[20] In this study, the size of the circular structure is around 20 μm, and no non-uniform platelets attachment or platelets aggregation was found, thus we think the uneven distribution also did not significantly affect the antithrombogenicity. Modifications of hydrogels by mixing with functional molecules has been extensively studied,[20, 21, 31] however, the main problem of physically mixing is the low stability. Slow leaching of the functional molecules from the grafts/scaffolds was shown [44] and will gradually decrease the activity of the biomolecule and change the mechanical properties of the material. To assess the stability of the fucoidan mixing modification presented in this study, we stored the PVA-F hydrogels for up to 2 months and measured the fucoidan density using toluidine blue staining. During the 2-month storage, minimal change of fucoidan concentration was found (Fig 1E). This is because that fucoidan was not only physically mixed into PVA hydrogels, but also chemically linked to PVA chain by the STMP crosslinking. STMP crosslinking of pullulan has been studied elsewhere, and the reaction mechanism has been proposed. [45, 46] Herein, we propose a similar crosslinking process as shown in Fig S11, and the phosphate assay proved the presence of phosphate crosslinking bonds in both PVA and PVA-F hydrogels (Fig 2A).

One of the main advantages of the STMP-crosslinked PVA for small diameter vascular grafts is their tunable mechanical properties. According to our previous studies, by adjusting the crosslinking density and fabrication parameters, we were able to fabricate PVA grafts with compliance up to 4.00±3.41%/40mmHg, [15, 16] matching that of rabbit carotid artery (3.1%/40mmHg) [47] and human brachial artery (1.3–3.3%/40mmHg) [48]. In this study, we examined the effect of fucoidan modification on the mechanical properties of PVA grafts. Results showed that the fucoidan modification did not alter the compliance of PVA grafts (Fig 2C). Furthermore, PVA-F grafts exhibited a higher crosslinking density compared to plain PVA as measured by phosphate density, further proving that fucoidan is not only physically mixed into PVA, but also chemically crosslinked to PVA through STMP. The higher crosslinking density of PVA-F also yielded stronger grafts with higher burst pressure (Fig 2D) and Young's modulus (Fig 2E and F).

Unmodified PVA does not support cells adhesion, and our previous studies have tried different modifications, including plasma treatment [17, 18] and incorporation of proteins and peptides to enhance endothelial cell adhesion.[20–22] Fucoidan was previously found to stimulate endothelial proliferation and potentiated endothelial cell growth and migration with the presence of fibroblast growth factor-1 (FGF-1).[13] Other studies also suggested that fucoidan binds to integrin $\alpha_M\beta_2$ and promotes the FGF-2-induced overexpression of integrin α_6 in human umbilical endothelial cells, which could further promote neovascularization.[49–52] In this study, after modifying PVA with fucoidan, HUVECs displayed a substantially enhanced adhesion on PVA-F, while without modification, PVA had minimal cell attachment, which was consistent to our previous observations.[19, 21] HUVECs on PVA-F and glass coverslips had similar densities and showed cobblestone morphology. Other than adhesion and spreading, endothelial cells are required to form into a tight-knit and confluent monolayer to maintain its function as a semipermeable barrier. Platelets/endothelial cell adhesion molecule-1 (PECAM1), also known as CD31, is expressed at endothelial cell-cell junctions, and is shown to be important to restore endothelial integrity.[53] Vascular endothelial cadherin (VE-cadherin) is an important type of adherens junctions, which is critical to control endothelial permeability and maintain cell-cell adhesion.[54] The HUVECs on PVA-F expressed strong CD31 and VE-Cadherin at the cell boundaries, indicating the integrity of endothelial cell monolayer. Endothelial nitric-oxide synthase (eNOS) is expressed in vascular endothelial cells and produces nitric oxide, which is known to regulate the vascular tone as well as smooth muscle cell proliferation.[55] HUVECs on PVA-F expressed eNOS, and the amount of eNOS is higher than HUVECs on glass cover slips. All of these cell marker expression measurements indicated that the HUVECs not only attached to the PVA-F surfaces, but also functioned as mature endothelial monolayers.

Hemocompatibility is an essential property of vascular grafts to prevent acute thrombosis formation after implantation. PVA has low platelets attachment and low thrombin generation, [20, 22] and fucoidan-modified PVA showed similar or slightly better hemocompatibility compared to plain PVA. We speculate that the good hemocompatibility was due to the ability of fucoidan to inhibit thrombin generation and platelets aggregation. Fucoidan has antithrombotic activity as tested in different *in vivo* models.[12, 55] It was found that the antithrombotic activity of fucoidan was mediated by heparin cofactor II,[41]

and fucoidan molecules inhibit thrombin generation by blocking the formation of intrinsic factor Xa.[40] Our real-time thrombin generation test observed slower and less thrombin generation on PVA-F compared to PVA samples (Fig 4C–F), supporting the antithrombotic activity of fucoidan. The fucoidan we used here is crude *fucus vesiculosus* fucoidan, with a molecular weight range from 20 kDa to 200 kDa and a sulfate content of 32% [56]. In previous studies, *fucus vesiculosus* fucoidan displayed anticoagulant properties, but did not prevent thrombin-induced platelet aggregation.[57] Durig et al. also found *fucus vesiculosus* fucoidan could induce irreversible platelet aggregation.[58] However, in our study, slightly more platelets were attached on PVA-F samples, but no platelet aggregation was observed (Fig 4A) after 1-hour incubation with rabbit platelet rich plasma. *Ex-vivo* shunt results in a non-human primate model also showed a low number of platelet and fibrin accumulation after 1-hour of whole blood flow with no antiplatelet or anticoagulant therapies (Fig 6).

Sterilization is required to remove micro-organisms before implantation, and gamma irradiation is one the most commonly used sterilization methods for biomaterial clinical use. Gamma irradiation is known to be able to cause chain scission,[59] and studies also found that gamma irradiation could cause branching and crosslinking,[60, 61] which combine to raise the concern that mechanical properties of the implants may be altered due to gamma sterilization. Our compliance and burst pressure measurement of PVA and PVA-F grafts before and after gamma sterilization did not show a significant difference (Fig S4). Previous studies also revealed that gamma irradiation changes the surface and biological properties of biomaterials.[62, 63] Srinivas *et al.*[62] found that gamma treated gels had a decreased surface hydrophilicity with increased dose, and cell adhesion and proliferation were found to be enhanced. A similar trend was observed from our PVA and PVA-F hydrogels. Although contact angle was not significantly increased (Fig S6), HUVEC density on gamma treated PVA-F hydrogels was significantly higher than non-gamma treated samples (Fig 5A–C and Fig S5). Denizli *et al.* showed that gamma irradiation drastically increased the blood protein adsorption on polycarbonate films, which could increase the risk of thrombus formation and platelet accumulation and activation.[64] Our studies also showed that after gamma irradiation, the thrombin generation was slightly increased for both unmodified PVA and PVA-F (Fig 5D–E). *Ex-vivo* shunt study also exhibited a slightly higher fibrin accumulation on gamma treated PVA-F (PVA-Fg) compared to non-gamma treated PVA-F, however, the difference was not significant, and the accumulation level was still lower than plain PVA (Fig 6). Overall, the *ex-vivo* shunt results were in line with the *in vitro* hemocompatibility test results that fucoidan modification did not increase platelets activation and thrombin generation, and gamma sterilization did not significantly change the hemocompatibility of PVA-F samples.

After confirming the *in vitro* and *ex vivo* performance of PVA-F, *in vivo* performance of PVA-F grafts was evaluated in a rabbit right carotid artery model with an end-to-side anastomotic technique. Previous studies have shown that when positioned in rabbit carotid artery with an end-to-end anastomosis, ePTFE grafts had a failure rate of 11.2% in the first 2 weeks due to thrombotic occlusion, or lost patency after 16 weeks due to intimal hyperplasia formation.[65, 66] We observed similar results in our ePTFE implantation with end-to-side anastomosis. Occluded ePTFE was occluded by the time of first ultrasound detection at day 14, as shown in Fig S7, which was caused by thrombus formation, while patent ePTFE

remained good flow until the endpoint. Similarly, most unmodified PVA grafts occluded by day 14, which could also be due to the thrombus formation. Gamma sterilized PVA-F grafts (PVA-Fg) yielded a much higher patency rate (Fig 7B) and maintained a stronger flow after 1 month compared to PVAg grafts (Fig 7D and Fig S7), which could be benefitted from the endothelial cell attachment (Fig 8). In addition to endothelial coverage on the surface, low intimal hyperplasia formation is also essential to maintain long term patency. The anastomotic junctions of graft and artery are prone to generate intimal hyperplasia due to the abnormal smooth muscle cell proliferation and migration. In our study, the majority of the cells in the intimal hyperplasia regions of all types of implanted grafts was identified as smooth muscle cells (Fig 9D), however, the Ki67 staining showed that most of the smooth muscle cells were not in proliferating state (Fig 9E). Previous study reported the time course of cell proliferation in the intimal hyperplasia using an angioplasty model,[67] and found out that the cellular proliferation in the intimal hyperplasia largely subsided by day 14 after injury, which was in line with our observation that there were low number of proliferating cells in the intimal hyperplasia at one month after implantation. Fucoidan was shown to be a potent inhibitor of smooth muscle cell proliferation through inhibiting mitogen-activated protein kinase pathway in a similar manner as heparin. [14, 68] In our study, PVA-Fg grafts had a lower stenosis percentage at both proximal and distal anastomoses compared to PVAg grafts (Fig 9), which could be attributed to the inhibition effect of fucoidan on smooth muscle cell proliferation at an early stage after implantation. ePTFE grafts are the gold standards for large diameter vascular grafts, however, ePTFE grafts with small diameters are not suitable due to the frequent intimal hyperplasia formation and blood clotting. The ePTFE grafts with 2 mm diameter were included in this study as clinical controls, and most of the ePTFE grafts showed strong blood flow after 1-month implantation. However, significant intimal hyperplasia was observed on the ePTFE grafts and the patency varied from sample to sample. It is worth mentioning that the ePTFE grafts we used for implantation have thinner wall and porous structure compared to other clinical available ePTFE grafts as shown in Table S1. Although the performance of PVA-F grafts and ePTFE grafts cannot be compared due to the differences in grafts size and wall thickness, the ePTFE grafts are still valuable clinical controls.

This study has demonstrated that the fucoidan modification was capable to improve endothelialization and hemocompatibility of PVA, and also enhanced the *in vivo* performance of PVA small diameter vascular grafts.

Conclusions

This study presented a fucoidan modification on PVA hydrogels to enhance endothelialization and hemocompatibility. The presence of fucoidan on PVA substantially improves the endothelial cell adhesion and coverage on PVA while maintaining the hemocompatibility of PVA. The *in vivo* test of the fucoidan modified PVA small diameter grafts exhibited promising results with a higher patency rate and remarkably lower intimal hyperplasia formation. The study suggests the potential of fucoidan as surface modification molecule for small diameter PVA grafts as well as broader application to development of other vascular implants and devices.

Supplementary Material

Refer to Web version on PubMed Central for supplementary material.

Acknowledgements

This work was supported by NSERC-CREATE, Training in Global Biomedical Technology Research and Innovation at the University of Waterloo [CREATE Funding 401207296]; National Institutes of Health (NIH R01 HL130274-01A1, R01HL144113 and R01DE026170); and the Oregon National Primate Research Center NIH grant award [P51OD011092]. We acknowledge Dr. Filip Konecny, Ms. Grace Pohan, Ms. Sabrina Mattiassi, Ms. Rebecca Mac, Ms. Yejin Jeong and University of Waterloo Central Animal Facility for their help with animal study. We are grateful to Dr. Alfred Yu, Dr. Adrian Chee, Mr. Yat Shun Yiu and Mr. Hanyue Shangguan for technical assistance with ultrasound imaging. We also appreciate the contributions of Mr. Matthew Hagen, Ms. Jennifer Johnson, Ms. Tiffany Burch, and the ONPRC staff for their help in data collection and analysis of the shunt studies.

References

[1]. Bos GW, Poot AA, Beugeling T, van Aken WG, Feijen J, Small-Diameter Vascular Graft Prostheses: Current Status, Archives of Physiology and Biochemistry 106(2) (1998) 100–115. [PubMed: 9894866]

[2]. Bergan JJ, Veith FJ, Bernhard VM, Yao JST, Flinn WR, Gupta SK, Scher LA, Samson RH, Towne JB, Randomization of autogenous vein and polytetrafluoroethylene grafts in femoral-distal reconstruction, Surgery 92(6) (1982) 921–930. [PubMed: 6755789]

[3]. Pevec WC, Darling RC, L'Italien GI, Abbott WM, Femoropopliteal reconstruction with knitted, nonvelour Dacron versus expanded polytetrafluoroethylene, Journal of Vascular Surgery 16(1) (1992) 60–65. [PubMed: 1535669]

[4]. Zilla P, Bezuidenhout D, Human P, Prosthetic vascular grafts: Wrong models, wrong questions and no healing, Biomaterials 28(34) (2007) 5009–5027. [PubMed: 17688939]

[5]. Hiob MA, She S, Muiznieks LD, Weiss AS, Biomaterials and Modifications in the Development of Small-Diameter Vascular Grafts, ACS Biomaterials Science & Engineering 3(5) (2016) 712–723.

[6]. Hoshi RA, Van Lith R, Jen MC, Allen JB, Lapidos KA, Ameer G, The blood and vascular cell compatibility of heparin-modified ePTFE vascular grafts, Biomaterials 34(1) (2013) 30–41. [PubMed: 23069711]

[7]. Qiu X, Lee BL-P, Ning X, Murthy N, Dong N, Li S, End-point immobilization of heparin on plasma-treated surface of electrospun polycarbonate-urethane vascular graft, Acta Biomaterialia 51 (2017) 138–147. [PubMed: 28069505]

[8]. Dimitrievska S, Cai C, Weyers A, Balestrini JL, Lin T, Sundaram S, Hatachi G, Spiegel DA, Kyriakides TR, Miao J, Li G, Niklason LE, Linhardt RJ, Click-coated, heparinized, decellularized vascular grafts, Acta Biomaterialia 13 (2015) 177–187. [PubMed: 25463496]

[9]. Li B, Lu F, Wei X, Zhao R, Fucoidan: Structure and Bioactivity, Molecules 13(8) (2008).

[10]. Ale MT, Mikkelsen JD, Meyer AS, Important Determinants for Fucoidan Bioactivity: A Critical Review of Structure-Function Relations and Extraction Methods for Fucose-Containing Sulfated Polysaccharides from Brown Seaweeds, Marine Drugs 9(10) (2011).

[11]. Fernando IPS, Kim D, Nah J-W, Jeon Y-J, Advances in functionalizing fucoidans and alginates (bio)polymers by structural modifications: A review, Chemical Engineering Journal 355 (2019) 33–48.

[12]. Min S-K, Kwon O-C, Lee S, Park K-H, Kim J-K, An Antithrombotic Fucoidan, Unlike Heparin, Does Not Prolong Bleeding Time in a Murine Arterial Thrombosis Model: A Comparative Study of Undaria pinnatifida sporophylls and Fucus vesiculosus, Phytotherapy Research 26(5) (2012) 752–757. [PubMed: 22084059]

[13]. Giraux J-L, Matou S, Bros A, Tapon-Bretaudière J, Letourneur D, Fischer A-M, Modulation of human endothelial cell proliferation and migration by fucoidan and heparin, European Journal of Cell Biology 77(4) (1998) 352–359. [PubMed: 9930660]

[14]. Religa P, Kazi M, Thyberg J, Gaciong Z, Swedenborg J, Hedin U, Fucoidan Inhibits Smooth Muscle Cell Proliferation and Reduces Mitogen-activated Protein Kinase Activity, European Journal of Vascular and Endovascular Surgery 20(5) (2000) 419–426. [PubMed: 11112459]

[15]. Chaouat M, Le Visage C, Baille WE, Escoubet B, Chaubet F, Mateescu MA, Letourneur D, A Novel Cross-linked Poly(vinyl alcohol) (PVA) for Vascular Grafts, Adv. Funct. Mater 18(19) (2008) 2855–2861.

[16]. Cutiongco MF, Kukumberg M, Peneyra JL, Yeo MS, Yao JY, Rufaihah AJ, Le Visage C, Ho JP, Yim EK, Submillimeter Diameter Poly(Vinyl Alcohol) Vascular Graft Patency in Rabbit Model, Front Bioeng Biotechnol 4 (2016) 44. [PubMed: 27376059]

[17]. Pohan G, Chevallier P, Anderson DEJ, Tse JW, Yao Y, Hagen MW, Mantovani D, Hinds MT, Yim EKF, Luminal Plasma Treatment for Small Diameter Polyvinyl Alcohol Tubular Scaffolds, Frontiers in Bioengineering and Biotechnology 7(117) (2019).

[18]. Ino JM, Chevallier P, Letourneur D, Mantovani D, Le Visage C, Plasma functionalization of poly(vinyl alcohol) hydrogel for cell adhesion enhancement, Biomatter 3(4) (2013) e25414. [PubMed: 23989063]

[19]. Cutiongco MF, Goh SH, Aid-Launais R, Le Visage C, Low HY, Yim EK, Planar and tubular patterning of micro and nano-topographies on poly(vinyl alcohol) hydrogel for improved endothelial cell responses, Biomaterials 84 (2016) 184–95. [PubMed: 26828683]

[20]. Ino JM, Sju E, Ollivier V, Yim EK, Letourneur D, Le Visage C, Evaluation of hemocompatibility and endothelialization of hybrid poly(vinyl alcohol) (PVA)/gelatin polymer films, J Biomed Mater Res B Appl Biomater 101(8) (2013) 1549–59. [PubMed: 23846987]

[21]. Anderson DEJ, Truong KP, Hagen MW, Yim EKF, Hinds MT, Biomimetic modification of poly(vinyl alcohol): Encouraging endothelialization and preventing thrombosis with antiplatelet monotherapy, Acta Biomaterialia 86 (2019) 291–299. [PubMed: 30639349]

[22]. Cutiongco MF, Anderson DE, Hinds MT, Yim EK, In vitro and ex vivo hemocompatibility of off-the-shelf modified poly(vinyl alcohol) vascular grafts, Acta Biomater 25 (2015) 97–108. [PubMed: 26225735]

[23]. Marinval N, Morenc M, Labour MN, Samotus A, Mzyk A, Ollivier V, Maire M, Jesse K, Bassand K, Niemiec-Cyganek A, Haddad O, Jacob MP, Chaubet F, Charnaux N, Wilczek P, Hlawaty H, Fucoidan/VEGF-based surface modification of decellularized pulmonary heart valve improves the antithrombotic and re-endothelialization potential of bioprostheses, Biomaterials 172 (2018) 14–29. [PubMed: 29715592]

[24]. Purnama A, Aid-Launais R, Haddad O, Maire M, Mantovani D, Letourneur D, Hlawaty H, Le Visage C, Fucoidan in a 3D scaffold interacts with vascular endothelial growth factor and promotes neovascularization in mice, Drug Delivery and Translational Research 5(2) (2015) 187–197. [PubMed: 25787743]

[25]. Wang Y, Ye CR, Su H, Wang J, Wang YA, Wang HH, Zhao AS, Huang N, Layer-by-layer self-assembled laminin/fucoidan films: towards better hemocompatibility and endothelialization, Rsc Adv 6(61) (2016) 56048–56055.

[26]. Pohan Grace, Mattiassi Sabrina, Yao Yuan, Zaw Aung Moe, Anderson Deirdre, Cutiongco Marie, Hinds Monica, Yim Evelyn, Effect of ethylene oxide sterilization on polyvinyl alcohol hydrogel compared to gamma radiation, Tissue Eng. A 26(19) (2020) 1077–1090. 10.1089/ten.TEA.2020.0002.

[27]. Smith PK, Mallia AK, Hermanson GT, Colorimetric method for the assay of heparin content in immobilized heparin preparations, Analytical Biochemistry 109(2) (1980) 466–473. [PubMed: 7224172]

[28]. Gupta A, Johnston CM, Hinds MT, Anderson DE, Quantifying physical thrombus characteristics on cardiovascular biomaterials using microCT, Methods and Protocols (Unpublished results).

[29]. Anderson DEJ, Pohan G, Raman J, Konecny F, Yim EKF, Hinds MT, Improving Surgical Methods for Studying Vascular Grafts in Animal Models, Tissue Engineering Part C: Methods 24(8) (2018) 457–464. [PubMed: 29984616]

[30]. de Mel A, Jell G, Stevens MM, Seifalian AM, Biofunctionalization of Biomaterials for Accelerated in Situ Endothelialization: A Review, Biomacromolecules 9(11) (2008) 2969–2979. [PubMed: 18831592]

[31]. Ren X, Feng Y, Guo J, Wang H, Li Q, Yang J, Hao X, Lv J, Ma N, Li W, Surface modification and endothelialization of biomaterials as potential scaffolds for vascular tissue engineering applications, Chemical Society Reviews 44(15) (2015) 5680–5742. [PubMed: 26023741]

[32]. Tang C, Kligman F, Larsen CC, Kottke-Marchant K, Marchant RE, Platelet and endothelial adhesion on fluorosurfactant polymers designed for vascular graft modification, Journal of Biomedical Materials Research Part A 88A(2) (2009) 348–358.

[33]. Hersel U, Dahmen C, Kessler H, RGD modified polymers: biomaterials for stimulated cell adhesion and beyond, Biomaterials 24(24) (2003) 4385–4415. [PubMed: 12922151]

[34]. Hsu S.-h., Sun S.-h., Chen DC, Improved Retention of Endothelial Cells Seeded on Polyurethane Small-diameter Vascular Grafts Modified by a Recombinant RGD-containing Protein, Artificial Organs 27(12) (2003) 1068–1078. [PubMed: 14678420]

[35]. Begovac PC, Thomson RC, Fisher JL, Hughson A, Gällhagen A, Improvements in GORE-TEX® vascular graft performance by Carmeda® bioactive surface heparin immobilization, European Journal of Vascular and Endovascular Surgery 25(5) (2003) 432–437. [PubMed: 12713782]

[36]. Bosiers M, Deloose K, Verbist J, Schroë H, Lauwers G, Lansink W, Peeters P, Heparin-bonded expanded polytetrafluoroethylene vascular graft for femoropopliteal and femorocrural bypass grafting: 1-year results, Journal of Vascular Surgery 43(2) (2006) 313–318. [PubMed: 16476607]

[37]. Yao Y, Wang J, Cui Y, Xu R, Wang Z, Zhang J, Wang K, Li Y, Zhao Q, Kong D, Effect of sustained heparin release from PCL/chitosan hybrid small-diameter vascular grafts on anti-thrombogenic property and endothelialization, Acta Biomaterialia 10(6) (2014) 2739–2749. [PubMed: 24602806]

[38]. van Sambeek MRHM, Segeren CM, van Dijk LC, van Essen JA, Dippel DWJ, van Urk H, Endovascular Repair of an Extracranial Internal Carotid Artery Aneurysm Complicated by Heparin-Induced Thrombocytopenia and Thrombosis, Journal of Endovascular Therapy 7(5) (2000) 353–358. [PubMed: 11032253]

[39]. Thakur S, Pigott JP, Comerota AJ, Heparin-induced thrombocytopenia after implantation of a heparin-bonded polytetrafluoroethylene lower extremity bypass graft: A case report and plan for management, Journal of Vascular Surgery 49(4) (2009) 1037–1040. [PubMed: 19341891]

[40]. Nishino T, Fukuda A, Nagumo T, Fujihara M, Kaji E, Inhibition of the Generation of Thrombin and Factor Xa by a Fucoidan from the Brown Seaweed Ecklonia kurome, Thrombosis Research 96(1) (1999) 37–49. [PubMed: 10554083]

[41]. Church FC, Meade JB, Treanor RE, Whinna HC, Antithrombin Activity of Fucoidan - the Interaction of Fucoidan with Heparin Cofactor-Ii, Antithrombin-Iii, and Thrombin, J Biol Chem 264(6) (1989) 3618–3623. [PubMed: 2914965]

[42]. Kukumberg M, Yao Y, Goh SH, Neo DJH, Yao JY, Yim EKF, Evaluation of the Topographical Influence on the Cellular Behavior of Human Umbilical Vein Endothelial Cells, Advanced Biosystems 2(6) (2018) 1700217. [PubMed: 30766915]

[43]. Koh LB, Rodriguez I, Venkatraman SS, The effect of topography of polymer surfaces on platelet adhesion, Biomaterials 31(7) (2010) 1533–1545. [PubMed: 19945746]

[44]. Atlan M, Simon-Yarza T, Ino JM, Hunsinger V, Corte L, Ou P, Aid-Launais R, Chaouat M, Letourneur D, Design, characterization and in vivo performance of synthetic 2 mm-diameter vessel grafts made of PVA-gelatin blends, Sci. Rep 8 (2018).

[45]. Dulong V, Forbice R, Condamine E, Le Cerf D, Picton L, Pullulan–STMP hydrogels: a way to correlate crosslinking mechanism, structure and physicochemical properties, Polymer Bulletin 67(3) (2011) 455–466.

[46]. Lack S, Dulong V, Picton L, Cerf DL, Condamine E, High-resolution nuclear magnetic resonance spectroscopy studies of polysaccharides crosslinked by sodium trimetaphosphate: a proposal for the reaction mechanism, Carbohydrate Research 342(7) (2007) 943–953. [PubMed: 17303095]

[47]. Matsumoto T, Okumura E, Shirono T, Sho E, Masuda H, Sato M, Flow-Induced Changes in Dimensions and Mechanical Properties of Rabbit Common Carotid Arteries, JSME International Journal Series C Mechanical Systems, Machine Elements and Manufacturing 48(4) (2005) 477–483.

[48]. Salzer DA, Medeiros PJ, Craen R, Shoemaker JK, Neurogenic-nitric oxide interactions affecting brachial artery mechanics in humans: roles of vessel distensibility vs. diameter, American Journal of Physiology-Regulatory, Integrative and Comparative Physiology 295(4) (2008) R1181–R1187.

[49]. Zemani F, Benisvy D, Galy-Fauroux I, Lokajczyk A, Colliec-Jouault S, Uzan G, Fischer AM, Boisson-Vidal C, Low-molecular-weight fucoidan enhances the proangiogenic phenotype of endothelial progenitor cells, Biochemical Pharmacology 70(8) (2005) 1167–1175. [PubMed: 16153611]

[50]. Chabut D, Fischer A-M, Colliec-Jouault S, Laurendeau I, Matou S, Le Bonniec B, Helley D, Low Molecular Weight Fucoidan and Heparin Enhance the Basic Fibroblast Growth Factor-Induced Tube Formation of Endothelial Cells through Heparan Sulfate-Dependent α6 Overexpression, Molecular Pharmacology 64(3) (2003) 696. [PubMed: 12920206]

[51]. Matou S, Helley D, Chabut D, Bros A, Fischer A-M, Effect of fucoidan on fibroblast growth factor-2-induced angiogenesis in vitro, Thrombosis Research 106(4) (2002) 213–221. [PubMed: 12297128]

[52]. Sarlon G, Zemani F, David L, Duong Van Huyen JP, Dizier B, Grelac F, Colliec-Jouault S, Galy-Fauroux I, Bruneval P, Fischer AM, Emmerich J, Boisson-Vidal C, Therapeutic effect of fucoidan-stimulated endothelial colony-forming cells in peripheral ischemia, Journal of Thrombosis and Haemostasis 10(1) (2012) 38–48. [PubMed: 22066680]

[53]. Lertkiatmongkol P, Liao D, Mei H, Hu Y, Newman PJ, Endothelial functions of platelet/endothelial cell adhesion molecule-1 (CD31), Curr Opin Hematol 23(3) (2016) 253–259. [PubMed: 27055047]

[54]. Vestweber D, VE-Cadherin, Arteriosclerosis, Thrombosis, and Vascular Biology 28(2) (2008) 223–232.

[55]. Kwak K-W, Cho K-S, Hahn O-J, Lee K-H, Lee B-Y, Ko J-J, Chung K-H, Biological effects of fucoidan isolated from Fucus vesiculosus on thrombosis and vascular cells, Korean J Hematol 45(1) (2010) 51–57. [PubMed: 21120163]

[56]. Fitton JH, Stringer DN, Karpiniec SS, Therapies from Fucoidan: An Update, Mar Drugs 13(9) (2015) 5920–5946. [PubMed: 26389927]

[57]. Cumashi A, Ushakova NA, Preobrazhenskaya ME, D'Incecco A, Piccoli A, Totani L, Tinari N, Morozevich GE, Berman AE, Bilan MI, Usov AI, Ustyuzhanina NE, Grachev AA, Sanderson CJ, Kelly M, Rabinovich GA, Iacobelli S, Nifantiev NE, and I on behalf of the Consorzio Interuniversitario Nazionale per la Bio-Oncologia, A comparative study of the anti-inflammatory, anticoagulant, antiangiogenic, and antiadhesive activities of nine different fucoidans from brown seaweeds, Glycobiology 17(5) (2007) 541–552. [PubMed: 17296677]

[58]. Dürig J, Bruhn T, Zurborn K-H, Gutensohn K, Bruhn HD, Béress L, ANTICOAGULANT FUCOIDAN FRACTIONS FROM FUCUS VESICULOSUS INDUCE PLATELET ACTIVATION IN VITRO, Thrombosis Research 85(6) (1997) 479–491. [PubMed: 9101640]

[59]. Ouano AC, Johnson DE, Dawson B, Pederson LA, Chain scission efficiency of some polymers in γ-radiation, Journal of Polymer Science: Polymer Chemistry Edition 14(3) (1976) 701–711.

[60]. Otaguro H, de Lima LFCP, Parra DF, Lugão AB, Chinelatto MA, Canevarolo SV, High-energy radiation forming chain scission and branching in polypropylene, Radiation Physics and Chemistry 79(3) (2010) 318–324.

[61]. Sáfrány Á, Beiler B, László K, Svec F, Control of pore formation in macroporous polymers synthesized by single-step γ-radiation-initiated polymerization and cross-linking, Polymer 46(9) (2005) 2862–2871.

[62]. Srinivas A, Ramamurthi A, Effects of Gamma-Irradiation on Physical and Biologic Properties of Crosslinked Hyaluronan Tissue Engineering Scaffolds, Tissue Engineering 13(3) (2007) 447–459. [PubMed: 17518597]

[63]. Matuska AM, McFetridge PS, The effect of terminal sterilization on structural and biophysical properties of a decellularized collagen-based scaffold; implications for stem cell adhesion, Journal of Biomedical Materials Research Part B: Applied Biomaterials 103(2) (2015) 397–406.

[64]. Denizli FK, Güven O, Competitive adsorption of blood proteins on gamma-irradiated-polycarbonate films, Journal of Biomaterials Science, Polymer Edition 13(2) (2002) 127–139. [PubMed: 12022745]

[65]. Cassel WS, Mason RA, Campbell R, Newton GB, Hui JCK, Giron F, An Animal Model for Small-Diameter Arterial Grafts, Journal of Investigative Surgery 2(2) (1989) 181–186. [PubMed: 2487246]

[66]. Byrom MJ, Bannon PG, White GH, Ng MKC, Animal models for the assessment of novel vascular conduits, Journal of Vascular Surgery 52(1) (2010) 176–195. [PubMed: 20299181]

[67]. Geary Randolph L, Williams JK, Golden D, Brown Deanna G, Benjamin Marshall E, Adams Michael R, Time Course of Cellular Proliferation, Intimal Hyperplasia, and Remodeling Following Angioplasty in Monkeys With Established Atherosclerosis, Arteriosclerosis, Thrombosis, and Vascular Biology 16(1) (1996) 34–43.

[68]. Vischer P, Buddecke E, Different action of heparin and fucoidan on arterial smooth muscle cell proliferation and thrombospondin and fibronectin metabolism, Eur J Cell Biol 56(2) (1991) 407–414. [PubMed: 1802722]

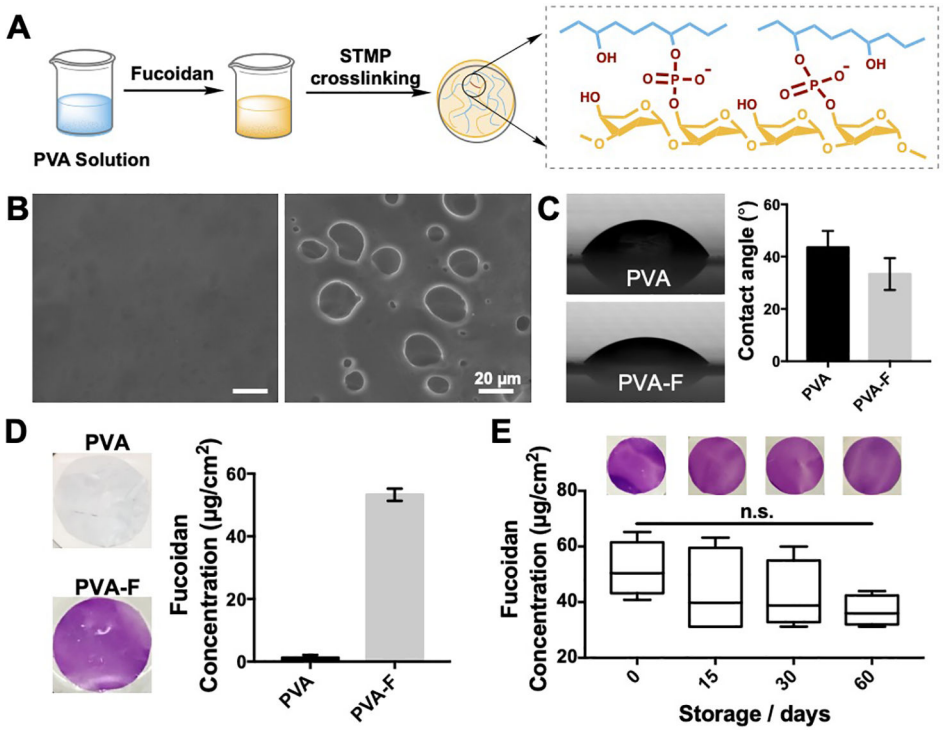

Figure 1.

(A) Schematic diagram of polyvinyl alcohol-fucoidan (PVA-F) preparation procedure. (B) Scanning electron microscopy (SEM) images showed the structures on PVA (left) and PVA-F (right) surfaces. (C) Static water contact angle of PVA and PVA-F surfaces. (n=6, p=0.0554). (D) Fucoidan density on PVA-F samples was determined by toluidine blue staining. (E) Stability of fucoidan modification was determined by toluidine blue staining at day 0, 15, 30 and 60. n=3, no significant decrease was observed.

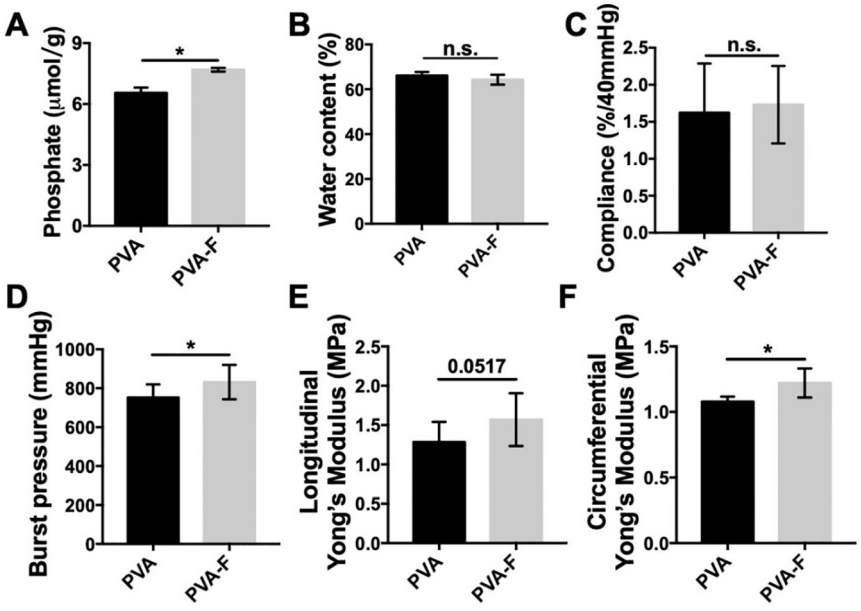

Figure 2.

Mechanical properties of PVA and PVA-F samples. (A) Crosslinking density of PVA-F samples is significantly higher than PVA samples (n=5). (B) Water content of PVA and PVA-F hydrogels (n=3). (C) Compliance of PVA and PVA-F samples (n=3). (D) Burst pressure of PVA and PVA-F samples (n=5). (E) Longitudinal tensile Young's modulus of PVA and PVA-F samples (n=3). (F) Circumferential tensile Young's modulus of PVA and PVA-F samples (n=3). * denotes statistical significance using t-test with $p < 0.05$, n=3.

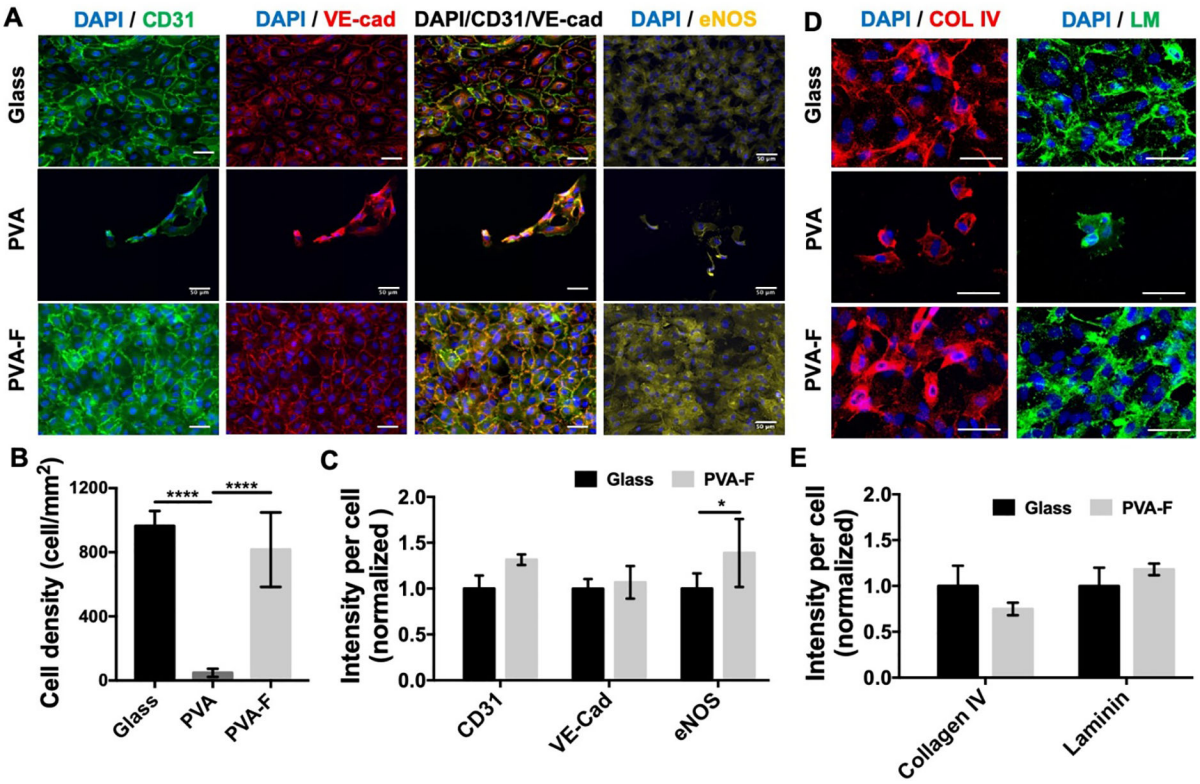

Figure 3.

Endothelial cell adhesion on PVA and PVA-F samples. (A) Representative fluorescence images of human umbilical vein endothelial cells (HUVECs) on PVA and PVA-F samples after 48 hr culture. Scale bar = 50 μm. (B) Average cell density on PVA and PVA-F samples. **** denotes statistical significance using one-way ANOVA with $p < 0.0001$, n=5. (C) CD31, VE-cadherin and eNOS expression of HUVEC monolayer on PVA-F samples (data normalized to glass). HUVECs on glass cover slip were included in analysis as a positive control. HUVECs on PVA samples were not taken into analysis. * denotes statistical significance using t-test with $p < 0.05$, n=5. (D) Representative fluorescence images of collagen type IV (COL IV) and laminin (LM) deposited by HUVECs on PVA and PVA-F samples after 24 hr culture samples (data normalized to glass). HUVECs on glass cover slip were included in analysis as a positive control. Scale bar = 50 μm. (E) Collagen type IV and laminin expression of HUVECs on PVA-F samples (data normalized to glass). HUVECs on PVA samples were not taken into analysis due to low cell number. No statistical significance was observed, n=3.

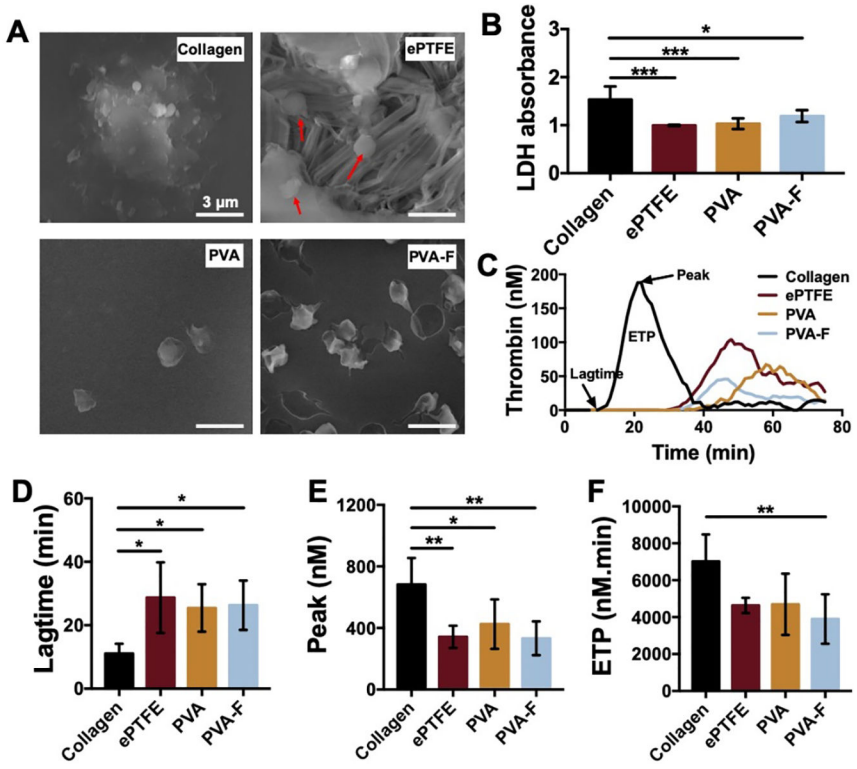

Figure 4.

In vitro hemocompatibility tests of PVA and PVA-F samples. (A) Platelet adhesion and morphology on collagen coated glass cover (positive control), ePTFE (clinical control, platelets are as indicated with arrows), PVA and PVA-F. (B) Quantification of platelet adhesion determined by lactate dehydrogenase (LDH) assay. (C) Real-time thrombin generation assay. Lag-time (D) represents the time taken to start forming thrombin. Peak (E) represents the maximum thrombin generation rate. (F) represents endogenous thrombin potential (ETP). n=5, *, **and *** indicate a significant difference using one-way ANOVA with $p < 0.05$, $p < 0.01$, and $p < 0.001$, respectively.

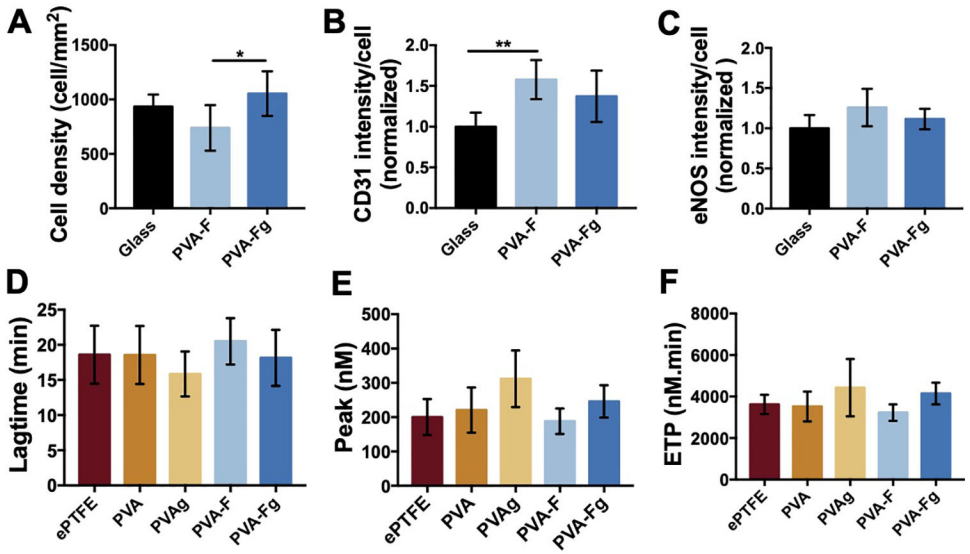

Figure 5.

Gamma sterilization effect on PVA-F samples. (A) Average cell density on PVA-F samples non-treated (PVA-F) and gamma sterilized (PVA-Fg). CD31 (B) and eNOS (C) expression of HUVECs on before and after gamma sterilized PVA-F sample (data normalized to glass). n=5, * and ** denotes statistical significance using one-way ANOVA with $p < 0.05$ and $p < 0.01$, respectively. Lagtime (D), Peak (E) and ETP (F) of real-time thrombin generation on non-treated and gamma sterilized samples (n=3).

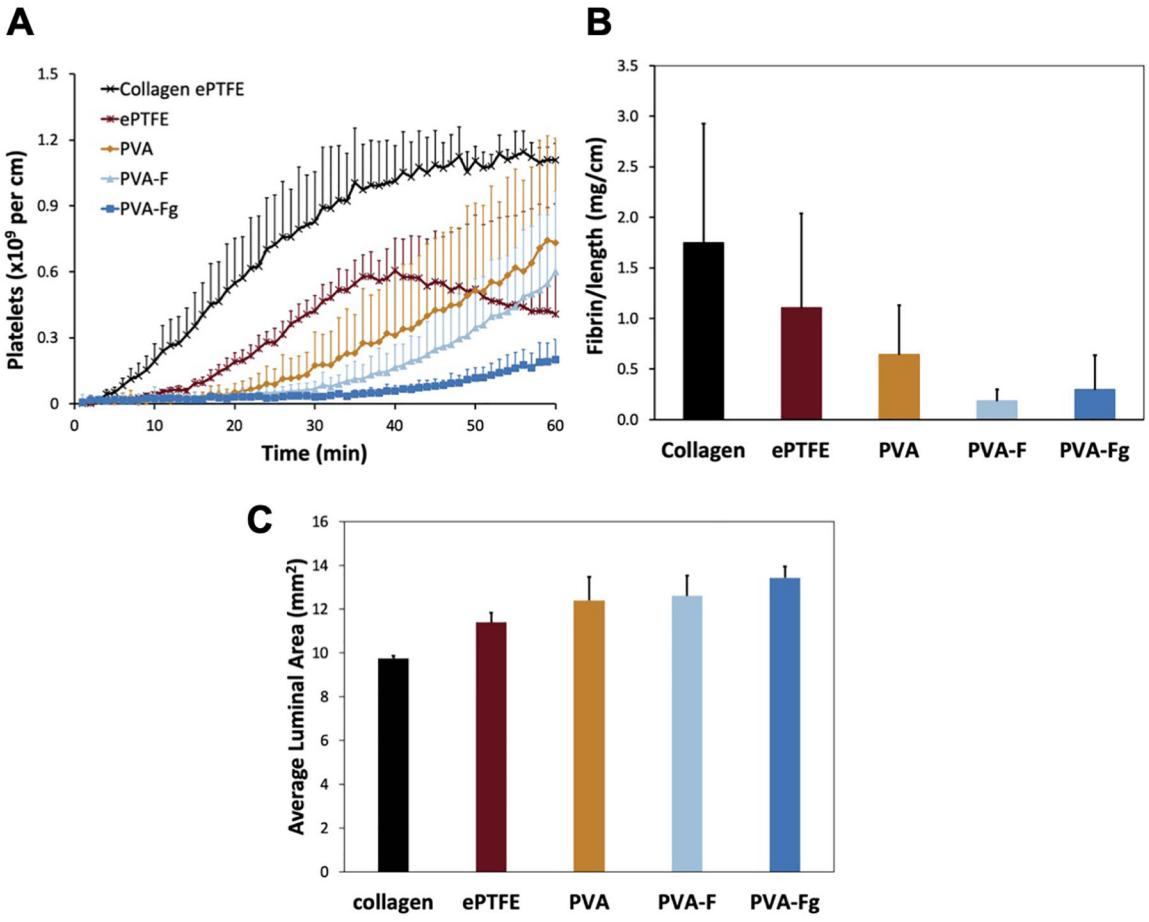

Figure 6.

Ex-vivo shunt study. Platelet accumulation (A), fibrin accumulation (B) and average luminal patent area (C) data are displayed as mean ± SD for all samples. Collagen and ePTFE controls are shown for comparison but were not included in the statistical comparison due to low sample size. No significant differences were observed between the various PVA samples for the platelet ($p=0.0523$), fibrin ($p=0.201$ for the 1-way ANOVA), or patent area ($p=0.109$ for the 1-way ANOVA) data.

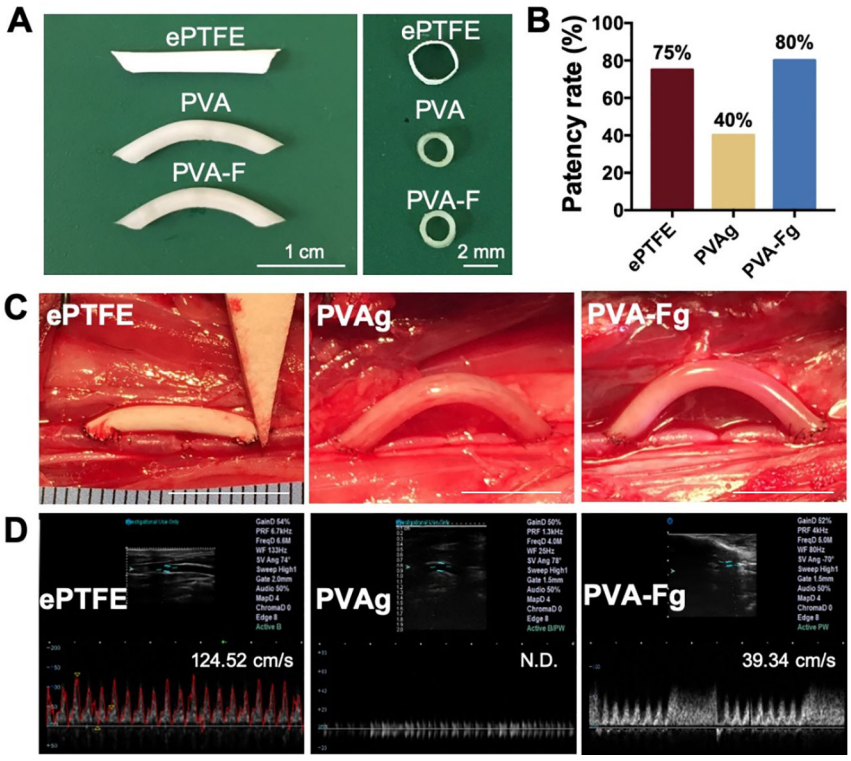

Figure 7.

Implantation of ePTFE, PVAg, and PVA-Fg grafts. (A) Dimensions of implanted grafts. (B) Patency rate of ePTFE (n=4), PVAg (N=5), and PVA-Fg (n=5). (C) Representative images of ePTFE graft, PVAg graft, and PVA-Fg graft after implantation. Scale bar=1cm. (D) Representative ultrasound images of ePTFE, PVAg, and PVA-Fg grafts and flow velocity (peak systolic velocity) inside the grafts after 1-month implantation. (N.D. not determined)

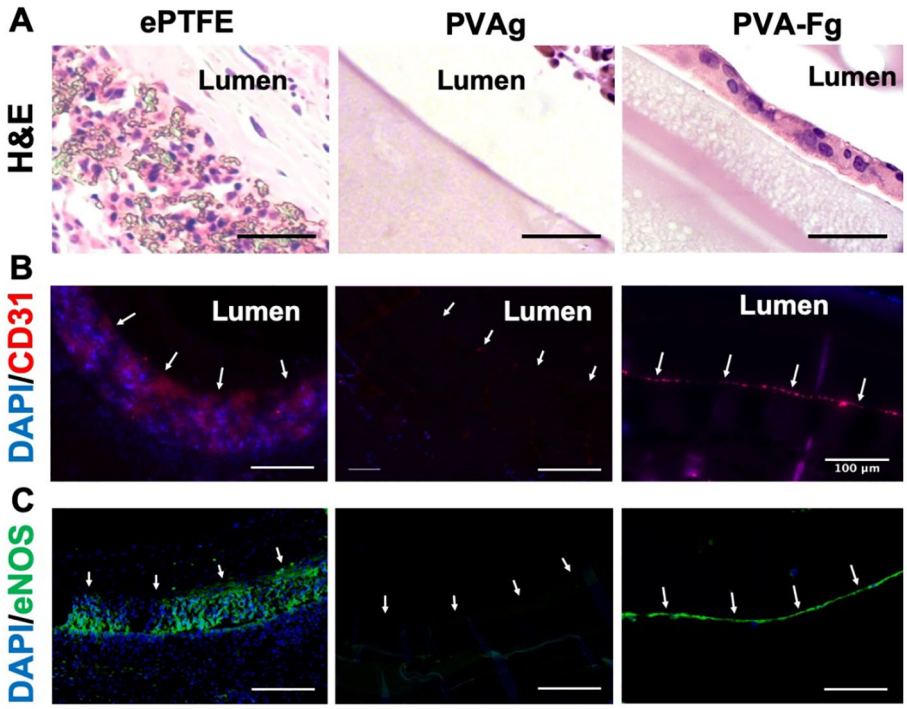

Figure 8.

In-vivo endothelialization of PVA-Fg grafts. (A) Hematoxylin and eosin (H&E) staining of middle section of explanted vascular grafts. PVA-Fg showed a layer of cells on the luminal surfaces. Scale bar = 50 μm. (B) Immunofluorescence staining of the middle section of explanted vascular grafts. Arrows indicate luminal surfaces. Scale bar = 100 μm. CD31 positive signals in PVA-Fg samples indicated the presence of endothelial cells. (C) Immunofluorescence staining of the middle section of explanted vascular grafts. Arrows indicate luminal surfaces. Scale bar = 100 μm. The eNOS positive signals indicated that the endothelial cells inside PVA-Fg samples expressed eNOS proteins.

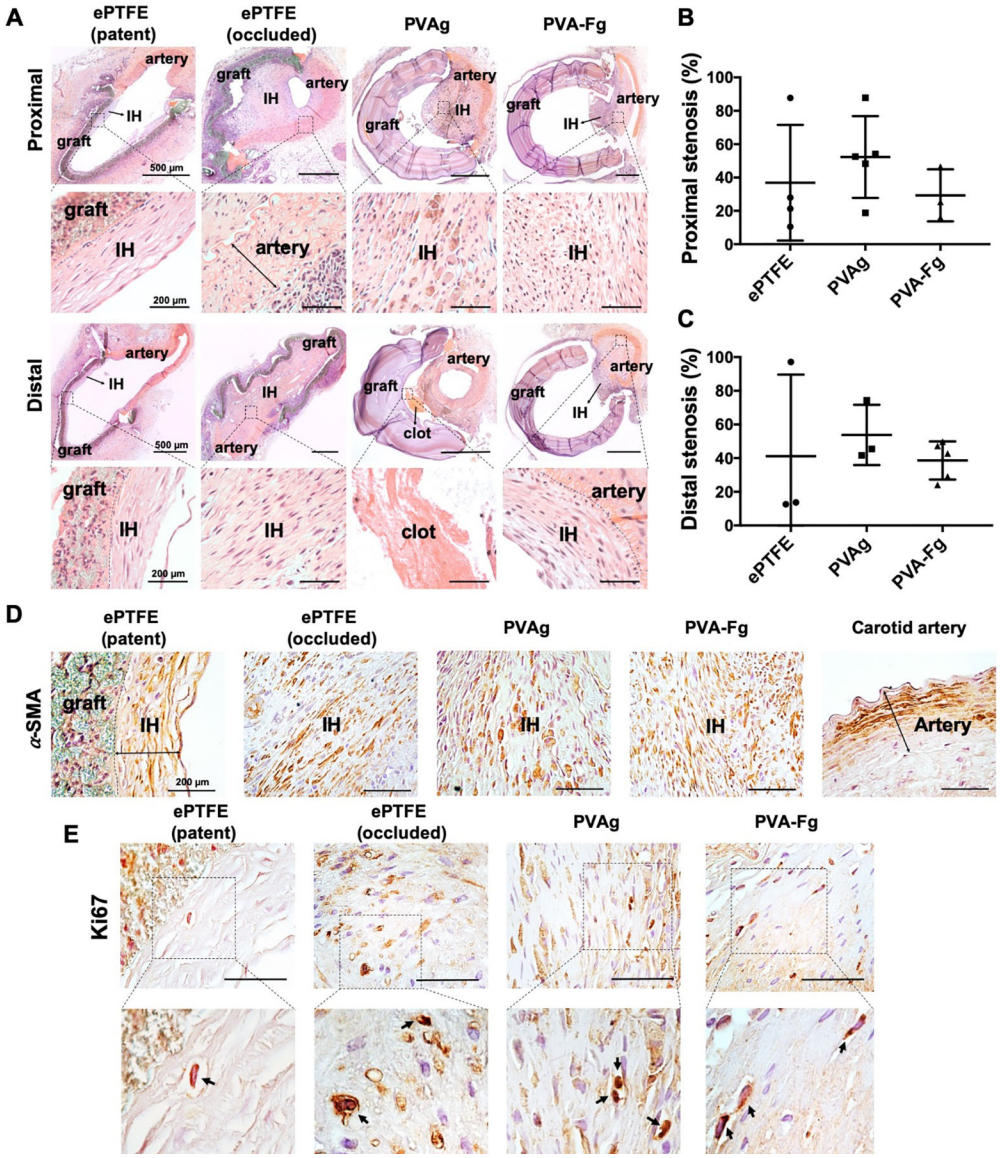

Figure 9.

Proximal and distal anastomotic stenosis of ePTFE, PVAg, and PVA-Fg grafts. (A) Representative H&E staining images of patent ePTFE, occluded ePTFE, PVAg, and PVA-Fg grafts. IH indicates intimal hyperplasia. (B) Stenosis percentage of ePTFE, PVAg, and PVA-Fg grafts at proximal anastomoses. (C) Stenosis percentage of ePTFE, PVAg, and PVA-Fg grafts at distal anastomoses. (Graft sections with missing pieces were not taken into calculation.) PVA-Fg grafts showed lower percentage of stenosis at both proximal and distal anastomosis than unmodified PVAg grafts. (D) α-SMA staining of patent ePTFE, occluded ePTFE, PVAg and PVA-Fg grafts confirmed the presence of smooth muscle cells in the intimal hyperplasia. Scale bar=200 μm. (E) Ki67 staining of patent ePTFE, occluded ePTFE, PVAg and PVA-Fg grafts showed the presence of proliferating cells, but in a low density. Scale bar=50 μm.